Obtaining geologically conformable tomographic models through anisotropic diffusion preconditioning

Zhijiang Luo, Dian Fan, Paul Farmer, Gary Martin, ION Geophysical*

Summary

Tomography driven model building workflow is currently pushing for increasingly higher resolution in the subsurface model. One key challenge in doing this is significant under-illumination in the model space due to fine inversion grids used. The poor illumination boosts data errors and introduces inversion artifacts into the solution, thus seriously degrading the resolution and accuracy of inverted models. To mitigate this issue, we propose to incorporate anisotropic diffusion smoothing operators into the conjugate gradient algorithm to precondition tomography. Synthetic and real examples demonstrate that this preconditioning can produce more detailed and structurally conformable velocity models than the conventional regularization-based tomography. Thus, we believe that the new approach is a valuable addition to the imaging workflow to derive high resolution velocity models for seismic imaging.

Introduction

Reflection tomography solves a linearized inversion system to find a subsurface model that best flattens reflection events picked on common image point gathers (Jones et al., 2007; Woodward et al., 2008; Luo et al., 2014). Today, tomography technology continues advancing to meet increasing production needs for building highly detailed and structure-following velocity models.

One big challenge in driving high resolution tomography is linked to the use of inversion grids whose order of sizes must match or be smaller than spatial wavelengths of velocity anomalies of interest. For example, the inversion grids as small as 10-25 m vertically and 100 m laterally have been used to resolve localized velocity heterogeneities (Fruehn et al., 2014). When such fine grids are adopted, ray illumination density per grid point is likely to diminish, and correspondingly, an increasing portion of the model space may become under-illuminated. This would result in a large null space in the model space, making the inversion problem highly ill-posed. If this issue is not treated properly, tomographic solutions will suffer from undesired inversion imprints such as ray illumination footprints, high wavenumber velocity noises and/or spurious velocity anomalies (Figure 1). In practice, various regularization and preconditioning techniques are used to suppress these artifacts by imposing additional constraints to the originally ill-posed problem and reducing the null space of the tomographic operator (VanDecar and Snieder, 1994; Clapp 2005; Zdraveva et al., 2013). The reconditioning of the problem is often designed with some smoothing operators that take no accounts of edge-preserving issue. Consequently, the tomographic inversion is able to remove inversion artifacts nicely but suffers from the loss of structural details in the model.

In this paper, we seek to precondition the inverse problem via anisotropic diffusion operators to produce tomographic solutions that are reasonably smooth but also rich in structural details. We apply the new method to both synthetic and real datasets, and compare the results with those from a conventional regularization-based tomography.

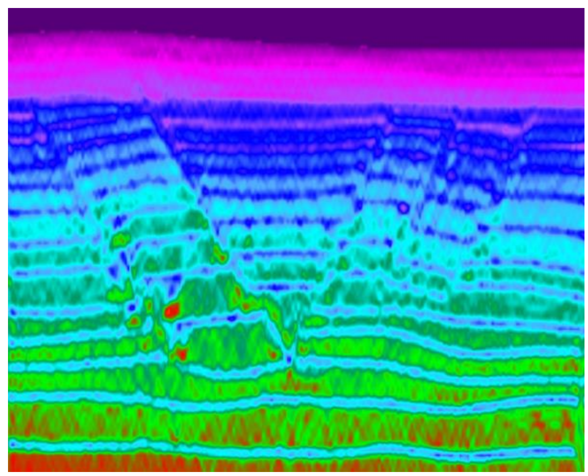

Figure 1: Raw tomographic velocity model produced when neither regularization nor preconditioning is applied. Note strong ray illumination imprints.

Method

A least square solution to the linearized tomography system is obtained by iteratively solving the normal equation system of the form

$$A^T A m = A^T d, \tag{1}$$

using the conjugate gradient (CG) algorithm. Here d is the measurements of residual moveouts, m is model perturbation, and A is Frechet derivatives mapping the model perturbation to the data.

Consider a left preconditioned system to (1) with some operator *P*, and the resulting CG algorithm will be slightly modified as follows (e.g., Saab, 2000):

$$\begin{aligned} \alpha &= \frac{z_i^T r_i}{(Ap_i)^T (Ap_i)} \\ m_{i+1} &= m_i + \alpha p_i \\ r_{i+1} &= r_i - \alpha A^T (Ap_i) \\ z_{i+1} &= P r_{i+1} \\ p_{i+1} &= z_{i+1} + \frac{z_{i+1}^T r_{i+1}}{z_i^T r_i} p_{i,} \end{aligned} \tag{2}$$

where r is the residual for normal equation system, z the preconditioned residual, p the search direction, and α the step length. It is clear from the algorithm (2) that the preconditioning merely applies operator P to explicitly change the CG search directions in the search for next solution move. Hence by incorporating prior information about the model into the preconditioner, we gain a direct way of shaping the search directions to guide the iterative inversion to converge to the desired solution.

A preconditioner can be any nonlinear mathematical operator or transformation that readily applies to an arbitrary vector (Saad, 2000). Anisotropic diffusion is a nonlinear partial differential equation operator and has received much attention in seismic industry for its edge-preserving smoothing capability ((Fehmers and Hocker, 2003; Hale, 2011). Here, we introduce a preconditioning approach driven by this operator as a way of suppressing inversion artifacts with the retention of structures details in-mind. With anisotropic diffusion, successive smoothed versions of an image $g(x)$ are generated by iteratively solving the following diffusive equation (e.g., Hale, 2011):

$$\frac{\partial g}{\partial t} = \nabla \cdot \varepsilon D \nabla g, \tag{3}$$

Here D is the diffusion tensor field and may be derived from the eigen-decomposition of structural tensors of a 3D seismic image by

$$D = \sum_{i=1}^{3} s_i\, u_i u_i^T, \tag{4}$$

where subscripted u and s are the eigenvector of the structural tensors and smoothing weight, respectively. The smoothing behavior of the diffusion operator (3) is determined by the shape of the tensor D. Note that the operator is termed anisotropic because the smoothing amplitude at each location differs in different directions. By changing the weights s, we can adapt the diffusive process to enforce strong smoothing along the dominant orientations of stratigraphic layering while inhibiting smoothing in the perpendicular direction. ε in the equation (3) represents a scalar field that can be used to put additional control over the diffusive behavior. For example, a depth varying ε enables the smoothing to be adapted to wavelength variations of seismic velocities.

In contrast to preconditioning, the regularization to the linearized tomographic problem is achieved by adding additional equations to inject physical constraints into the inversion. Note that the regularization does not directly modify the CG search directions. For 3D structure-guided tomography, one decent choice is the directional Laplacian operator that imposes the constraint of the form:

$$\sum_{i=1}^{3} s_i\, u_i^T H u_i = 0, \tag{5}$$

where u and s have the same meaning as in the equation (4), and H is the Hessian matrix of the image $g(x)$. The operator essentially minimizes second derivatives along the direction u, and is anisotropic as well.

Examples

The two tomography approaches are first tested using a synthetic layered model with complex embedded faults. This model is well suited for checking how well a tomographic algorithm can remove inversion artifacts with a minimal blurring of sharp velocity boundaries. The starting model used to generate PSDM gathers is a pretty smoothed version of the true model (Figure 2a), with all stratigraphic and structural details removed. Dense general moveout picks are made on the CRP gathers and brought into our generalized-moveout (GMO) tomography engine (Luo et al., 2014) for model reconstruction. Figure 2 compares the updated velocity models after one iteration of tomographic inversions. Both approaches reasonably recover the stratigraphy layering and fault traces of the true model, and the remigrated results confirm image focusing is greatly improved. Clearly, the model from the preconditioned version features better intra-layer lateral smoothing, and the detected faults are strikingly sharper and clearer (Figure 2c).

Figure 3 shows three snapshots of incremental model perturbations (i.e., a scaled version of search directions) after different CG iterations. As noted, the search directions under preconditioning are spatially smoother and more uniform than under regularization, indicating the explicit smoothing mechanism by preconditioning is more effective in shaping the search directions than regularized tomography. Also indicated is the extremely sharp fault traces seen in the search direction field with preconditioning than with regularizing, which contributes to the clear fault image in the final solution. Finally, significantly larger increment model perturbations are produced at early CG iterations (Figure 3, top right) with preconditioned tomography than regularized tomography, indicating preconditioning may boost the convergence rate of the solution.

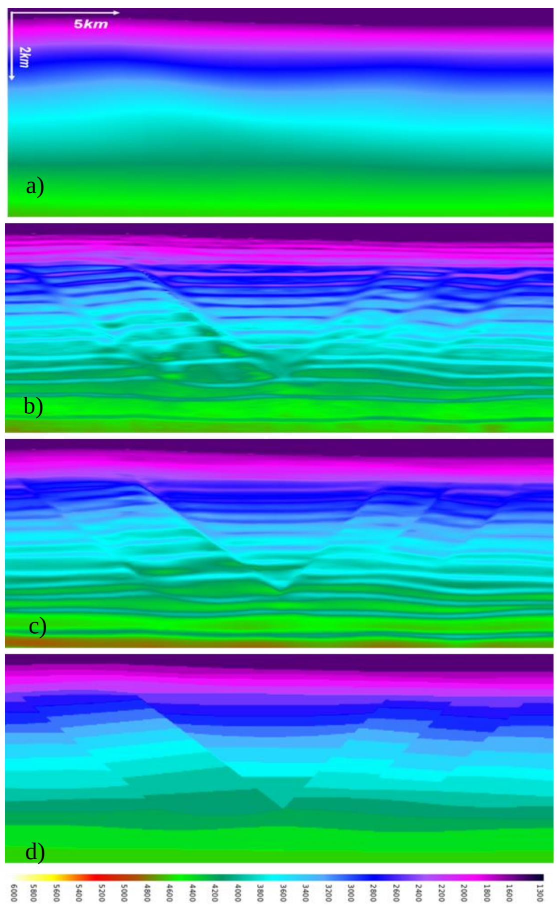

Figure 2. Velocity models in synthetic dataset tests: (a) Initial model, (b) Regularized tomography, (c) Preconditioned tomography and (d) True model.

Next, we apply the two approaches to a 2D field marine dataset acquired in offshore Guyana. The area is characterized by deformed stratigraphy layering that are displaced by numerous faults at various depths. The initial PSDM gathers are generated by Kirchhoff migration using a fairly smooth initial model. Figure 4 shows the velocity models after one iteration of GMO tomographic inversion. We can see that both approaches produce structuralized velocity updates and significantly enhance imaging quality when compared to the initial model. However, the anisotropic diffusion driven tomography generates more geology-following and detailed velocity updates than the regularized one. On the remigrated PSDM stacks (figure 5), we can see that with the preconditioned tomography, the reflectors are imaged more continuous and natural, and the faults are well resolved with reduced fault shadow distortion.

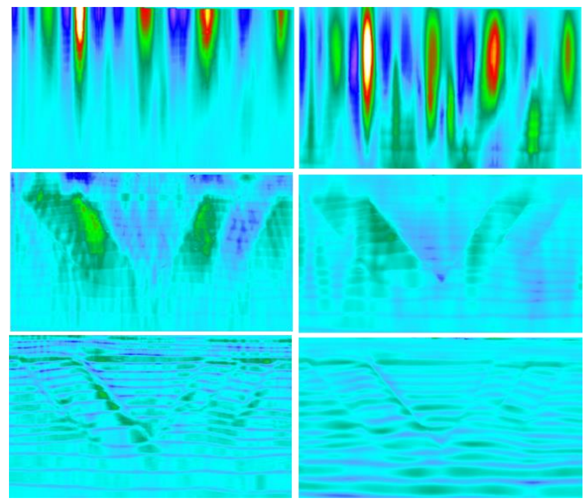

Figure 3: Incremental model perturbations (search directions multiplied by step length) after 1, 10, and 50 CG iterations (ordered from top to bottom). Left column for regularized tomography and right for preconditioned tomography.

Conclusion

High resolution tomography enables to build structurally conformable velocity models but is prone to suffer from inversion artifacts. The preconditioning technique allows an iterative solver to explicitly modify the CG search directions at each iteration. For this reason, we implement a preconditioning tomography via anisotropic diffusion to check if this helps to mitigate inversion artifacts and boost structural conformity of the solution. Both synthetic and field examples demonstrate its superior capability of generating structure-rich smoothed tomographic solutions when compared to the conventional structure-guided tomography.

Acknowledgements

We would like to thank Ian Jones and Jacques Leville for their reviews, Juergen Fruhen, Stuart Greenwood, Chong Chung and Brent Mecham for their valuable discussions and feedbacks. Finally, we thank ION Geophysical management for permission to publish this work.

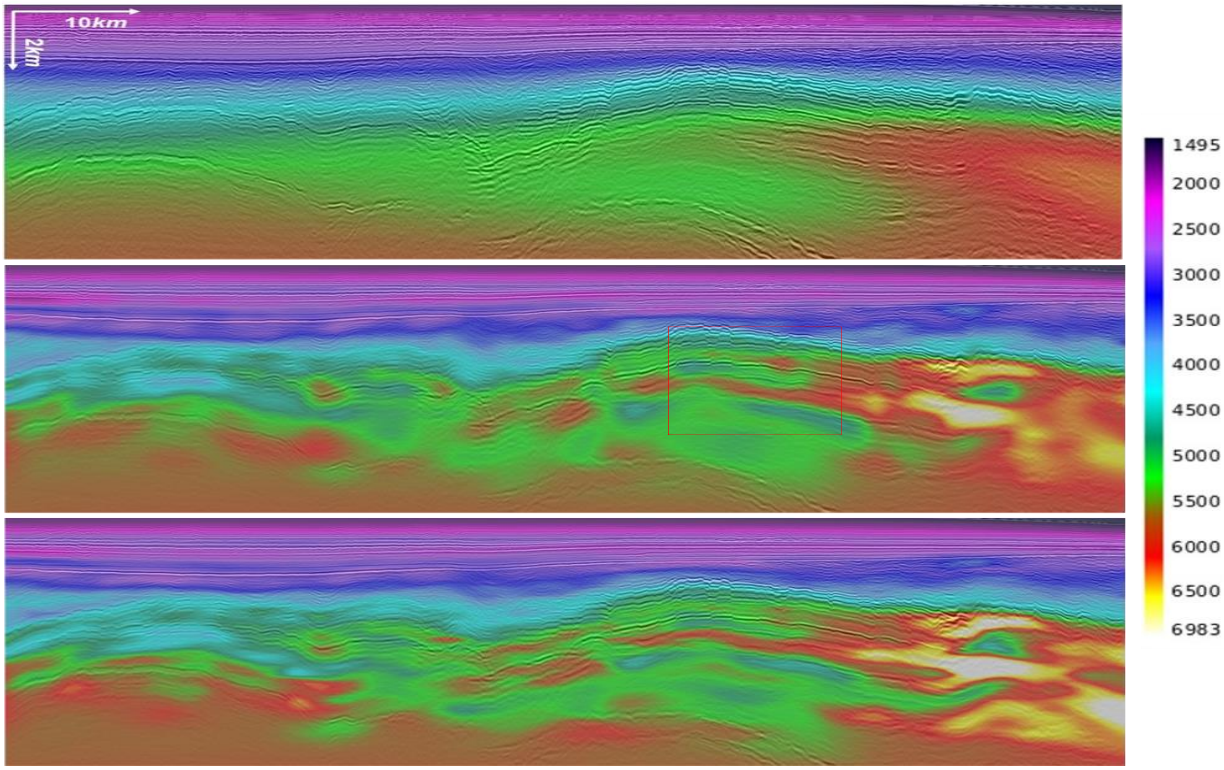

Figure 4: Velocity models overlaid onto PSDM seismic stacks on a marine field dataset: initial model (top), regularized tomography (middle) and preconditioned tomography (bottom). Red box indicates the area where PSDM stacks shown in Figure 5 are located.

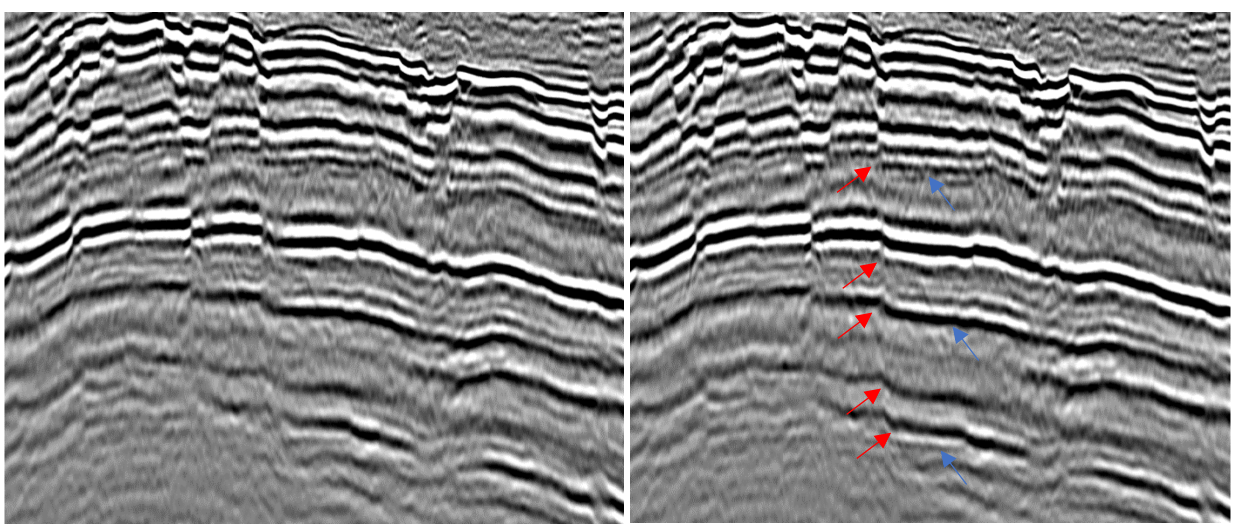

Figure 5: PSDM stacks remigrated using regularized tomography model (left) and preconditioned tomography model (right). Red arrows point to the clearly imaged fault; Blue arrows indicate reflectors being imaged more continuous and natural.

EDITED REFERENCES

Note: This reference list is a copyedited version of the reference list submitted by the author. Reference lists for the 2017 SEG Technical Program Expanded Abstracts have been copyedited so that references provided with the online metadata for each paper will achieve a high degree of linking to cited sources that appear on the Web.

REFERENCES

Clapp, R. G., B. L. Biondi, and J. F. Claerbout, 2004, Incorporating geologic information into reflection tomography: Geophysics, **69**, no. 2, 533–546, http://dx.doi.org/10.1190/1.1707073.

Fehmers, G.C., and C.F.W. Hocker, 2003, Fast structural interpretations with structure-oriented filtering: Geophysics, **68**, 1286–1293, http://dx.doi.org/10.1190/1.1598121.

Fruehn, J., V. Valler, N. Stevens, S. Adhikari, M. Phani, S. Sarkar, C. G. Rao, P. Kumar, and P. Routray, 2014, Velocity model update via inversion of non-parametric RMO picks over canyon areas offshore Sri Lanka: 84th Annual International Meeting, SEG, Expanded Abstracts, 3070–3074, http://dx.doi.org/10.1190/segam2014-0050.1.

Hale, D., 2009, Structure-oriented smoothing and semblance: CWP Report, 635.

Jones, I. F., M. J. Surgue, and P. B. Hardy, 2007, Hybrid gridded tomography: First Break, **25**, 15–21, http://dx.doi.org/10.3997/1365-2397.2007013.

Luo Z., J. Brittan, D. Fan, B. Mecham, P. Farmer, and G. Martin, 2014, Imaging complexity in the earth — Case studies with optimized ray tomography: The Leading Edge, **33**, 1016–1022, http://dx.doi.org/10.1190/tle33091016.1.

Saab, Y., 2003, Iterative methods for sparse linear systems (2nd ed): SIAM.

Vandecar, J., C., and R., Snieder, 1994, Obtaining smooth solutions to large, linear inverse problems: Geophysics, **59**, 818–829, http://dx.doi.org/10.1190/1.1443640.

Woodward, M. J., D. Nichols, O. Zhdraveva, P. Whitfield, and T. Johns, 2008, A decade of tomography: Geophysics, **73**, no. 5, VE5–VE11, http://dx.doi.org/10.1190/1.2969907.

Zdraveva, O., S., Hydal, and M., Woodward, 2013, Tography with geological constraints: an alternative solution for resolving carbonates: 83th Annual International Meeting, SEG, Expanded Abstracts, 4770–4774.